

Identifying the sources and geochemical evolution of groundwater using stable isotopes and hydrogeochemistry in the Quaternary aquifer in the area between Ismailia and El Kassara canals, Northeastern Egypt

Muhammad Gomaah¹ · Thomas Meixner² · E. A. Korany³ · Hassan Garamoon³ · Mohamed A. Gomaah¹

Received: 6 July 2015 / Accepted: 28 March 2016 / Published online: 14 May 2016
© Saudi Society for Geosciences 2016

Abstract The potential sources of recharge of both water and solutes to the Quaternary aquifer in the area between Ismailia and El Kassara canals in northeastern Egypt include seepage from the irrigation canals and conduits, return flow after irrigation in the cultivated fields, local precipitation, and the upward flow of groundwater from the underlying Miocene aquifer system. Water isotopes, solute concentrations, and sulfate isotopes were used to investigate the geochemical sources, reactions, and the impacts of the hydraulic connections among recharge sources. The obtained results indicate a minimal influence of the underlying Miocene aquifer as a water and solute source while old and new contributions from the irrigation canals represent the main sources of recharge. The chemical reactions responsible for the chemical constituents and salinity in the aquifer include silicate weathering, evaporite dissolution, and carbonate precipitation. Most of groundwater samples appear to lie at/or close to equilibrium with montmorillonite, kaolinite, and illite where clay minerals are quite common in the local soils of the Quaternary aquifer.

Keywords Stable isotopes · Hydrochemistry · Surface water–groundwater interaction · El Salhia El Giddida area

Introduction

Quaternary aquifers are of great importance for reclaimed land projects in arid and semi-arid regions like Egypt where The Nile water supply is not sufficient to meet all demands for the agricultural activities, and groundwater resources represent the alternative supply. El Salhia El Giddida occupies one of the new reclaimed projects using groundwater for irrigation purposes. Many hydrological, hydrochemical, and stable isotope studies have been conducted in and nearby the study area (El Dairy 1980; Salluma 1983; Salem 1996; Hamza et al. 1987; Al-Gamal et al. 2005; Salem and Sadek 2006; Dahab et al. 2007 and Ahmed et al. 2013). These studies indicated the presence of old Nile water and mixing between recent Nile with old Nile in most of the localities, yet they did not study the sources of groundwater for the study area in detail. Also they did not study the different geochemical reactions responsible for the chemical constituents. The chemical composition of groundwater is controlled by many factors that include composition of precipitation, geological structure, and mineralogy of the watersheds and aquifers. The interaction of all these factors leads to various water compositions (Murray 1996; Rosen and Jones 1998).

Tracing groundwater by means of environmental isotopes offer unique and supplementary information on the origin and movement of groundwater and its dissolved solutes and allows a quantitative evaluation of mixing and other physical processes such as evaporation and isotopic exchange in geologic systems (Mook 2000).

✉ Muhammad Gomaah
muhammad_gomaah@yahoo.com

Thomas Meixner
tmeixner@email.arizona.edu

E. A. Korany
akorany@hotmail.com

¹ Department of Hydrogeochemistry, Desert Research Center, Cairo, Egypt

² Department of Hydrology and Water Resources, University of Arizona, Tucson, AZ, USA

³ Department of Geology, Ain Shams University, Cairo, Egypt

The inverse geochemical modeling is commonly used to illustrate and reconstruct the chemical evolution of groundwater along a flow path from an initial point in an aquifer to a final point along a groundwater flow path (Sharif et al. 2008). The soundness and validity of inverse modeling results depends on a valid conceptualization of the groundwater system, the validity of basic concepts of aqueous geochemistry, accuracy of data, and an understanding of geochemical processes occurring in an aquifer (Güler and Thyne 2004).

To better understand the hydrological and geochemical properties of the aquifer system, we sought to answer three main questions in detail, which are as follows:

- What are the sources of groundwater to this aquifer?
- What chemical reactions are responsible for the chemical constituents and salinity?
- Is there any connection between the Quaternary aquifer and the underlying Miocene aquifer, and if so, to what degree?

In order to answer these questions, stable isotope ratios of $^2\text{H}/^1\text{H}$ and $^{18}\text{O}/^{16}\text{O}$ were used to identify the possible sources of recharge to the groundwater system and zones of mixing. Also, the dual isotope approach of $\delta^{34}\text{S}$ and $\delta^{18}\text{O}$ of sulfate was used to identify sulfate sources. A Na^+ -normalized Ca^{++} versus HCO_3^- and Na^+ versus Cl^- plots was used to identify the potential geochemical reactions controlling the chemical evolution and salinity of the groundwater in the Quaternary aquifer. Additionally, stability field diagrams of the $\text{Na}_2\text{O}-\text{SiO}_2-\text{Al}_2\text{O}_3-\text{H}_2\text{O}$, $\text{K}_2\text{O}-\text{SiO}_2-\text{Al}_2\text{O}_3-\text{H}_2\text{O}$ and $\text{CaO}-\text{SiO}_2-\text{Al}_2\text{O}_3-\text{H}_2\text{O}$ systems were used to identify the secondary clay minerals produced from the geochemical weathering of silicate minerals. Inverse model (Netpath-win) was also used to identify the geochemical reactions along two flow paths in the study area.

The area of study is located to the east of the Nile Delta, between Ismailia Canal to the south and El Kassara canal to the north. It is bounded by latitudes $30^\circ 32' 24$ and $30^\circ 40' 12$ N and longitudes $31^\circ 49.2'$ and $32^\circ 11.4'$ E (Fig. 1). It is characterized by a hot summer and a short rainy winter. The relative humidity is higher in winter than in summer, and evaporation intensity is generally higher in summer than that in winter. Annual rainfall ranges between 4.2 and 37 mm/year (Dahab et al. 2007) across the study site.

Geologic setting

The Quaternary aquifer in the studied area is composed of aeolian and old deltaic deposits which consist of sand and sandstone with intercalations of clay (Moussa 1990). The sedimentary succession in the study area is strongly affected by faulting and folding processes (El Dairy 1980) which are dominantly represented by NE–SW normal faults with

downthrown side towards southeast and northwest and NW–SE normal faults with strike dip towards northeast direction. The vertical displacement along these faults ranges from a few meters to hundreds of meters (Gad 1995). The western and middle parts are strongly affected by deep-seated normal faults where saline water of Miocene aquifer moves upward along the fault planes (Gad 1995).

Hydrogeological conditions

The Quaternary water bearing deposits rest directly on a Pliocene clay and Miocene sandy limestone (Fig. 2). The thickness of the Quaternary aquifer is strongly affected by a set of normal faults with downthrown sides towards the northeast. This faulting increases the aquifer thickness towards the north and northeast, where it ranges from 300 to 400 m in the study area while it reaches more than 900 m near the Mediterranean Sea. The Quaternary aquifer occurs under unconfined conditions. Semi-confined and confined conditions occur at the eastern and northeastern parts (East Abu Sweir area) of the aquifer. This pattern is attributed to the presence of shale and clay intercalation cap beds overlying the aquifer in these localities. Depths to groundwater show a wide range, with relatively large values at high elevations at the western and middle parts of the study area, ranging from 20 to 34 m below the ground surface. Depths to groundwater are small at the low topography areas representing the new reclaimed areas located northeast of Abu Sweir ranging from 6 m to less than one meter below the ground surface (Dahab et al. 2007) (Fig. 3).

Materials and methods

Field investigations were carried out during March and June 2013. A total of 103 water samples were collected at the head wells for chemical analyses. All wells had been in use before sampling until the pH and specific conductance stabilized to provide a representative in situ sample for groundwater. Physical parameters such as pH and EC were measured in the field. Samples were unfiltered and stored in pre washed propylene bottles thoroughly rinsed with the sample. The chemical analyses were performed after 5 days from collection with precision of less than 5 % E.B, at the hydrogeochemistry department, Desert Research Center, Cairo, Egypt. Alkalinity, calcium, magnesium, and chloride were analyzed by volumetric titration. Na and K were measured by a flame photometer (Jenway model PFP7). Nitrate, phosphate, and silica were analyzed by colorimetry with a UV–visible spectrophotometer (Thermo-Spectronic model 300). All the isotopic analyses were conducted at the University of Arizona Laboratory of Isotope Geo-chemistry. Deuterium and ^{18}O were measured on mass spectrometer

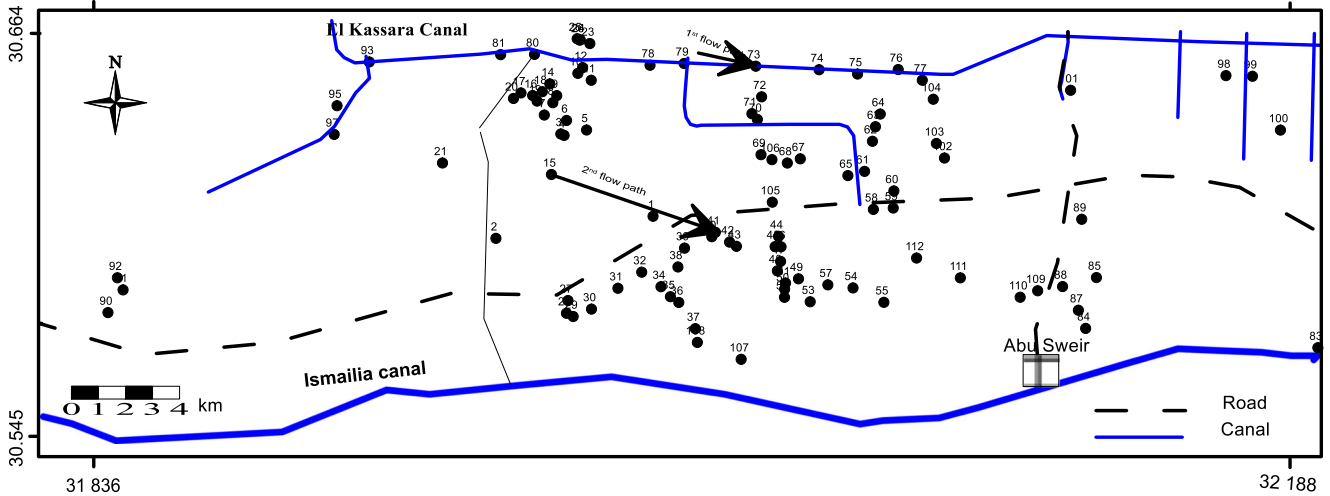


Fig. 1 Location map of samples site of the Quaternary aquifer at the study area

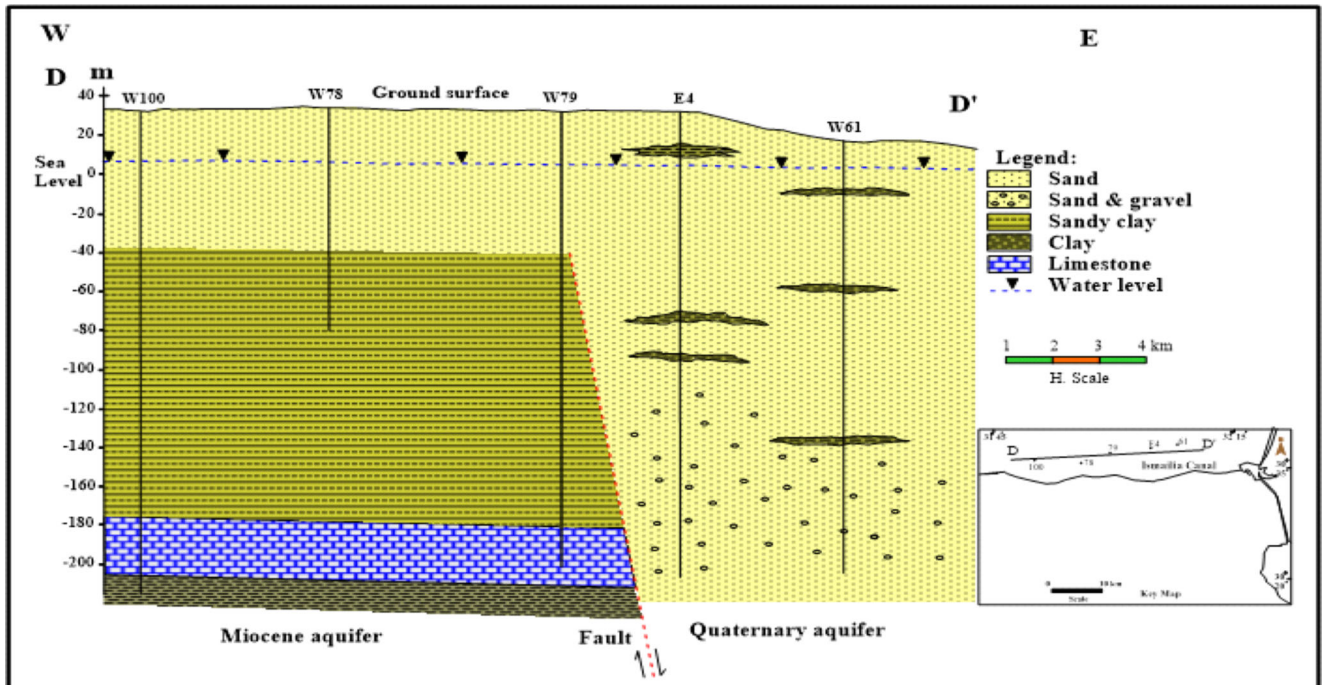


Fig. 2 Hydrogeological cross section DD', showing the composition of the Quaternary aquifer and the underlying aquifers (Dahab 2007)

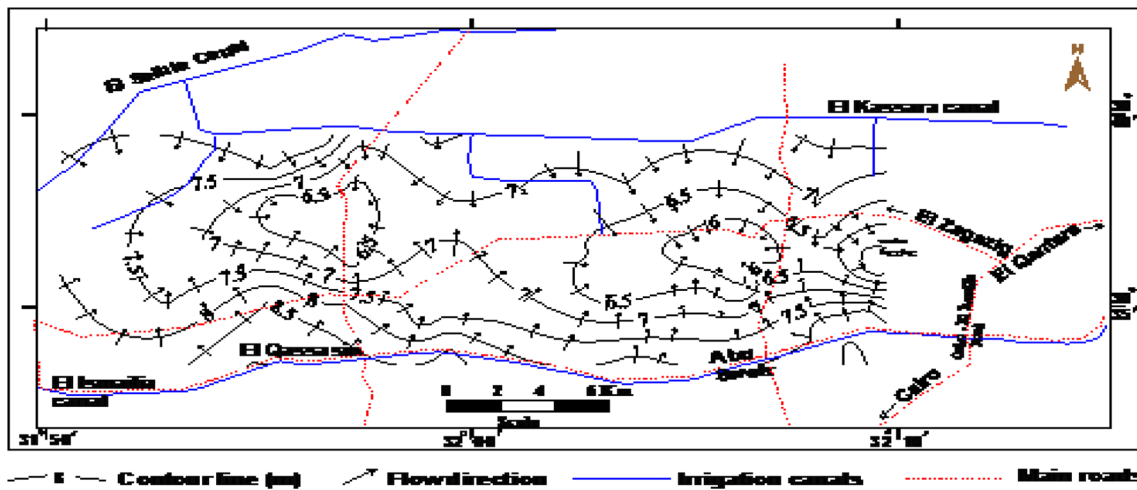


Fig. 3 Water levels and flow net map of the Quaternary aquifer in El Sahlia El Gidida–Abu Sweir area, east Delta, Egypt (Dahab 2007). It shows that the net flow is towards the middle of the study area

(Finnigan Delta S) with a precision of 0.9 per mil. $\delta^{34}\text{S}$ was measured on mass spectrometer (ThermoQuest Finnigan Delta PlusXL). $\delta^{18}\text{O}$ of sulfate was measured on mass spectrometer (Thermo Electron Delta V) with precisions estimated to be ± 0.15 or better.

NETPATH is a geochemical model that interprets the net geochemical mass balance reactions between the initial and final waters that accounts for the changes in the chemical and isotopic compositions along a hydrological flow path. The reactant phases used in mass-transfer modeling include the minerals determined by Moussa (1990) which are as follows: albite, orthoclase, microcline, muscovite, Na-montomorellinite, kaolinite, illite, chlorite, calcite, pyroxenes, amphiboles, and quartz.

Results and discussion

Stable isotopes

The stable isotope results reflect various mixing patterns between different water sources, namely fresh water from Ismailia canal and El Kassara canal with average values of $\delta^{18}\text{O}$ and $\delta^2\text{H}\%$ +3.426 and +24.48 ‰, respectively, and old Nile water prior to the construction of the Aswan High Dam with an average value of -0.6 and 4.3 for $\delta^{18}\text{O}$ and δD . The underlying Miocene paleowater has average values of -6.76 and -33 ‰ for $\delta^{18}\text{O}$ and $\delta^2\text{H}\%$ (Table 1). Mixing of these different kinds of water is clearly shown (Fig.4). Whenever contour lines of $\delta^{18}\text{O}$ and $\delta^2\text{H}\%$ show decreases in the direction of groundwater flow, recharge from surface water which is enriched in heavy stable isotopes and

Table 1 Results of the stable isotopes data

Sample ID	TDS	$\delta\text{O}\%$	$\delta^2\text{H}\%$
2	2706	1.827133	13.56336
3	1360.26	1.875123	12.21103
6	1168.2	1.902522	16.69909
9	1475.76	1.902938	17.29771
11	1234.2	1.928654	18.06511
14	1714.02	1.993788	15.47104
23	910.14	2.034125	17.50335
27	3260.4	2.131672	13.33273
28	3616.8	2.137896	13.22458
32	2923.8	2.149307	18.40871
35	2864.4	2.202505	12.85519
45	4144.8	2.315933	22.12533
49	4026	2.478815	17.13791
37	1107.48	2.311103	19.58815
61	466.62	2.479992	22.08942
70	859.98	2.554937	22.49765
71	1492.26	2.566233	21.96213
72	1128.6	2.60959	21.88853
73	480.48	2.645628	23.21864
74	436.92	2.664916	23.22724
75	564.3	2.682351	20.93445
77	601.26	2.769037	23.35646
83	1325.94	2.876888	23.40684
84	2303.4	3.405216	24.95645
90	3636.6	0.925515	8.846137
92	2310	0.936884	7.137008
93	2151.6	0.973456	8.753296
95	887.7	1.02516	9.626786
98	6072	1.290439	15.10232
99	2646.6	1.352449	11.07163
100	3300	1.367039	10.06842
101	2112	1.427613	13.28822
102	1980	1.485306	14.54187
103	2857.8	1.513617	14.61749
104	1127.28	1.515678	9.369336
107	3174.6	1.595912	18.32743
108	2158.2	1.802663	14.42324
Ismailia canal mean value	244	3.344256	25.33428
Miocene mean value (Al-Gamal et al. 2005)	4751	-1	-6
Old Nile mean value (Salem 1996)	200	-0.6	4.3

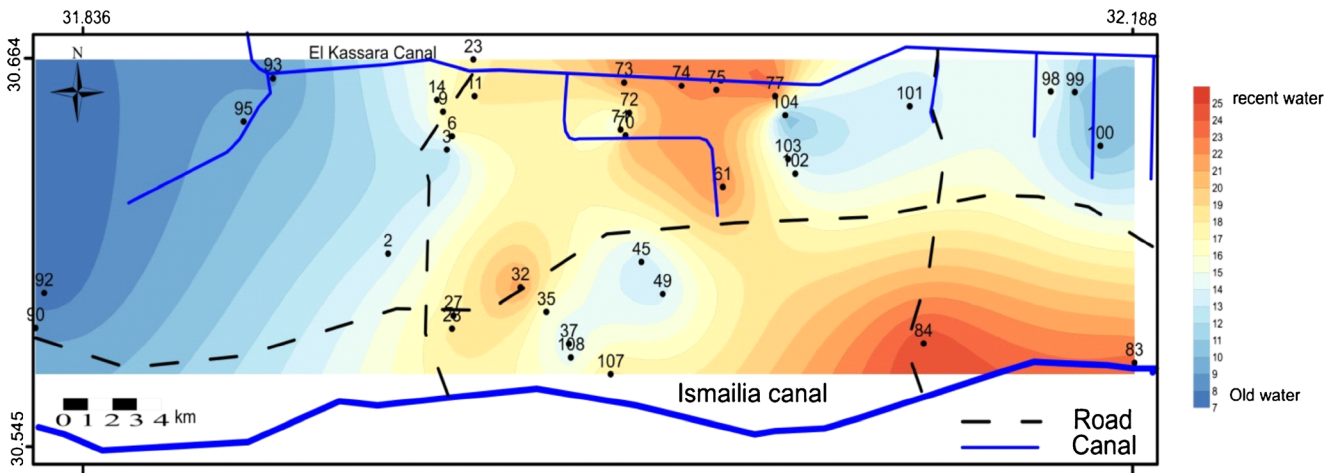


Fig. 4 Spatial distribution of $\delta^2\text{H}\text{‰}$ of the groundwater of the Quaternary aquifer reflecting various mixing patterns between different water sources, namely fresh water from Ismailia and El Kassara canals and old Nile water

Fig. 5 Plot of $\delta^{18}\text{O}\text{‰}$ versus $\delta^2\text{H}\text{‰}$, showing the meteoric origin of groundwater samples of the Quaternary aquifer. It is observed that both the surface water and some groundwater samples plot away from the LMWL showing evidence of isotopic enrichment by evaporation

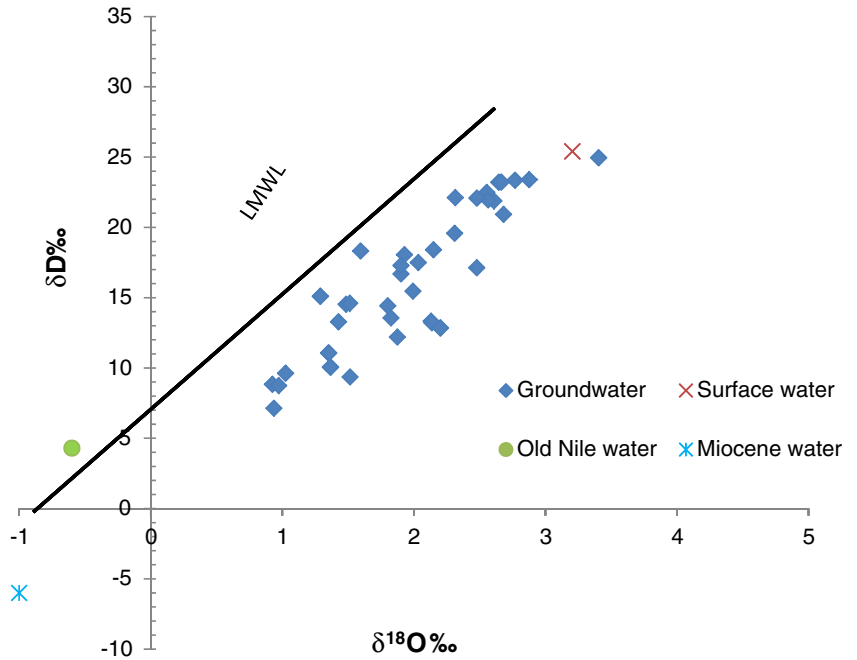


Fig. 6 The relationship between $\delta^{18}\text{O}\text{‰}$ versus chloride indicates three main types of water. The first group is waters in which leaching of salts lead to salinization, while the second group is those affected by both evaporation and leaching of salts together. The third group is those waters affected by the contribution of recharge from recent Nile water

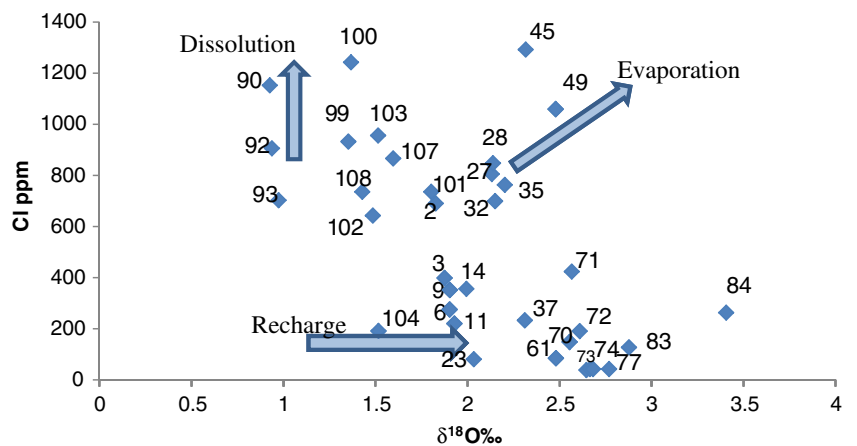
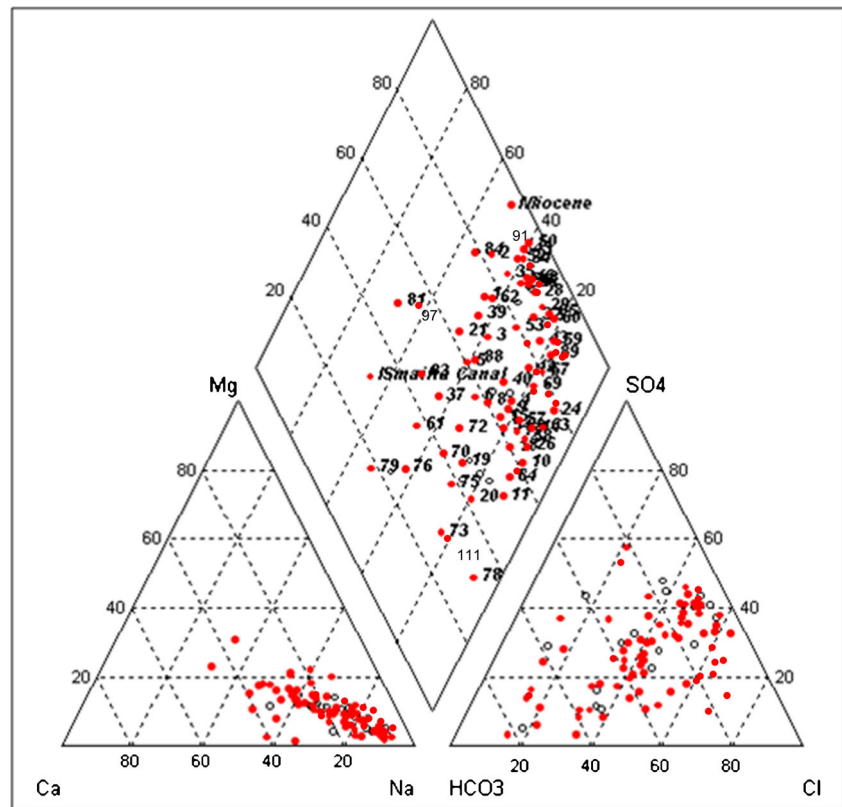


Fig. 7 Piper diagram which shows the different contributions of water sources from Recent Nile and Miocene aquifer



mixed with other water of less enriched heavy isotopic composition is occurring.

The most enriched water has $\delta^{18}\text{O}$ and $\delta^2\text{H}\text{‰}$ values equal to +3.4 and +24.95 ‰, respectively, which is located at the southeastern part of the study area. The enrichment is attributed to aridity conditions. On the other hand, it can be seen that the most depleted closed lines ($\delta^{18}\text{O}$ varies from +0.9 to 1.1 ‰ and $\delta^2\text{H}\text{‰}$ varies from +7 to +9 ‰) represent an isolated formation with low permeability which has remained away from recent recharge.

As evident from Fig. 5, most of the groundwater samples plot below the local meteoric water line (LMWL), suggesting a meteoric origin. It is observed that both the surface water and some groundwater samples plot away from the LMWL showing evidence of isotopic enrichment by evaporation on the surface or in the unsaturated zone before recharge. The relationship between $\delta^{18}\text{O}$ and Cl^- can interpret the geochemical mechanism of groundwater caused by the evaporation effect. If salinity is due to evaporation, a plot of

Fig. 8 The relationship between $\delta^{18}\text{O}\text{‰}$ versus the TDS, showing three different groups of groundwater of the Quaternary aquifer in the study area

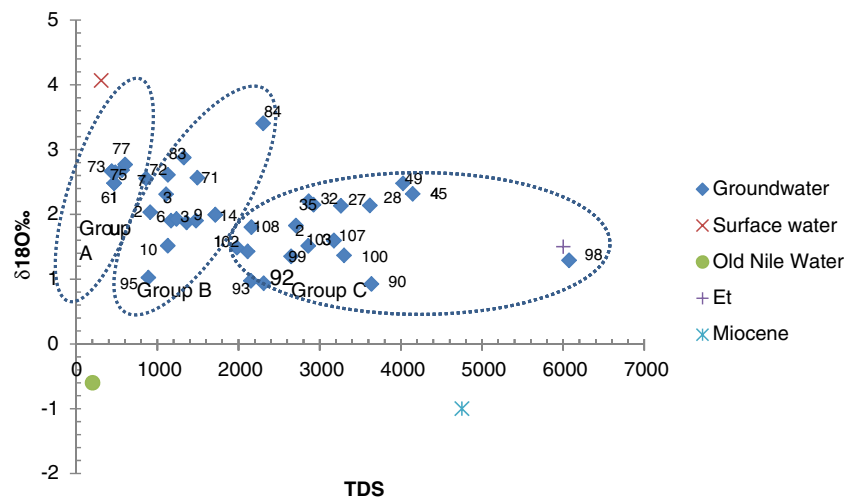
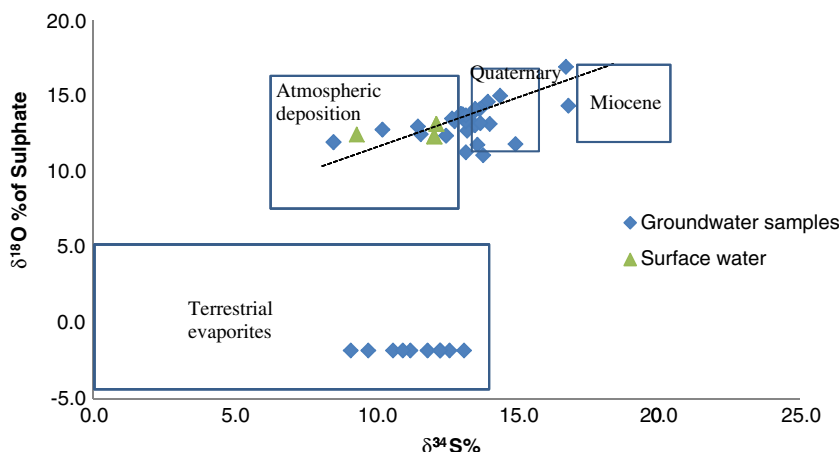


Fig. 9 The relationship between $\delta^{34}\text{S}_{\text{SO}_4\%}$ and $\delta^{18}\text{O}_{\text{SO}_4\%}$ showing three sources of sulfate, which are as follows: terrestrial evaporate, atmospheric deposition, and sulfate from the Quaternary and Miocene aquifer



chloride content or total dissolved solids against $\delta^{18}\text{O}$ or $\delta^2\text{H}\text{‰}$ will be positively correlated, as increased evaporation would result in isotopic enrichment as well as an increase in Cl^- . If salinity is due to leaching of evaporate salts by rapid percolation through preferential pathways, then groundwater should retain $\delta^{18}\text{O}$ or $\delta^2\text{H}\text{‰}$ similar to that of the original rainfall with high content of Cl^- or TDS. On the other hand, recharge from surface water would result an increase in heavy isotope content and low content of Cl^- . The relationship between $\delta^{18}\text{O}$ and Cl^- (Fig. 6) indicates three main types of water are observed. The first group is waters in which leaching of salts lead to salinization, while the second group is those affected by both evaporation and leaching of salts together. The third group are those waters affected by the contribution of recharge from recent Nile water.

Piper diagram is also a good tool to check the water sources along with stable isotopes. It shows that some groundwater samples are plot close to the surface water which indicates the contribution from recent Nile water (Fig 7), while few samples plot close to the Miocene water which reflects the contribution from the underlying Miocene aquifer. Piper diagram also shows that the majority of groundwater samples (76 %) lie in the sub area of Na–Cl water type, where primary salinity

exceeds 50 %. Twenty percent of the groundwater samples lie in the sub area of Na– HCO_3 . The rest of the samples lie in the subarea of Ca– HCO_3 water type.

Sources of groundwater and salinity

There are four poles of water and solutes sources in the study area; the old recharge by Nile water, recent recharge by Nile water, the Miocene water, and the evapotranspiration as shown in Fig. 8 which reveals that the major contribution is coming from a water whose O-18 is more or less homogenous with varying salinities due to dissolution of different minerals. In addition, three different groups of waters are recognized as the following:

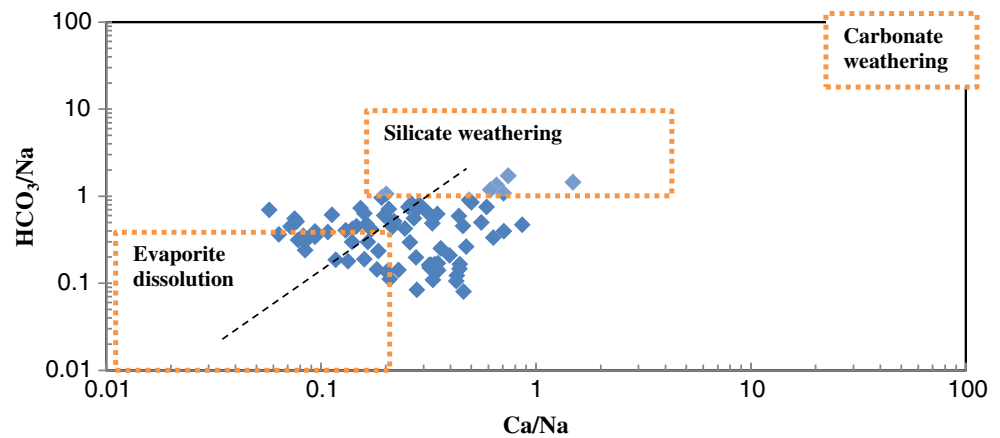
Group A (low TDS)

Samples of this group plot on the mixing line between the old recharge by Nile water (before construction of Aswan High Dam) and recent recharge by Nile water (Fig. 8). Location of each sample on this line indicates its relative degree of mixing. The isotopic content ranges between +1.02 and +2.76 ‰ with respect to $\delta^{18}\text{O}$ and +9.62 and +23.35 ‰ with respect to $\delta^2\text{H}\text{‰}$.

Table 2 Summary of simple arithmetic mean, max. and min. values of chemical analysis for groundwater

parameter	EC (µ/cm)	pH	Na (mg/l)	K (mg/l)	Ca (Mg/l)	Mg (mg/l)	Cl (mg/l)	HCO ₃ (mg/l)	SO ₄ (mg/l)	NO ₃ (mg/l)	SiO ₂ (mg/l)	
March and June 2013	<i>n</i>	104	104	102	102	102	102	102	102	102	102	
	Minimum	499	7.4	45	1	8	2	254	173	12	0	2
	Maximum	9200	8.84	1453	28	492	147	1800	660	1865	297	70
	Average	3162	8.18	532	8.3	120	41	549	382	529	55	27

Fig. 10 A Na normalized Ca VS HCO_3^- plot, showing that all group samples range from being influenced by silicate weathering to evaporite dissolution



The TDS ranges between 437 and 910 ppm, indicating short residence time.

Group B (moderate TDS)

This group includes samples which are deviated slightly from the mixing line of the recent old Nile water, suggesting an increase of salinity (1107 to 2100 ppm) due to leaching and dissolution of salts (Fig. 8). It shows an isotopic content ranging from +1.51 to +3.4 and +9.3 to +24.95 ‰ for $\delta^{18}\text{O}$ and $\delta^2\text{H}$ ‰, respectively.

Group C (high TDS)

Samples of group C plot between the four end members showing mixing of different sources. This group includes samples with an isotopic content ranging from +0.92 to +2.47 and +8.84 to +17.13 ‰ for $\delta^{18}\text{O}$ and $\delta^2\text{H}$ ‰, respectively. The TDS ranges from 2000 to 6000 ppm.

Sources of sulfates

Sulfate can be of atmospheric, pedospheric, and lithospheric origin. In addition, sulfate derived from anthropogenic sources, such as industrial wastes, fertilizers, and soil amendments. Commonly, their distinctive isotope compositions allow one to clearly distinguish the sulfur sources in the groundwater and surface water (Gu, 2005). The analysis of coupled $\delta^{34}\text{S}$ and $\delta^{18}\text{O}$ (SO_4) data concentrations reveal that there are three sulfate sources in groundwater (Fig. 9). The first sulfate source is from the terrestrial sulfate, where $\delta^{34}\text{S}$ values vary from 9.1 to 13.1 ‰; ^{18}O (SO_4) values are -1.8 ‰. Bacterial sulfate reduction results in a positive correlation of $\delta^{34}\text{S}$ and $\delta^{18}\text{O}$ with a slope near 1 (Clark and Fritz 1997); where bacteria catalyze this reaction, it is easier for bacteria to break ^{32}S -O bonds than ^{34}S -O bonds.



Fig. 11 Plot of the Na versus Cl relationship showing that some samples are along with the trend-line indicating halite dissolution while the majority plot above the 1:1 trend-line showing that silicate weathering is one of the sources of sodium ions

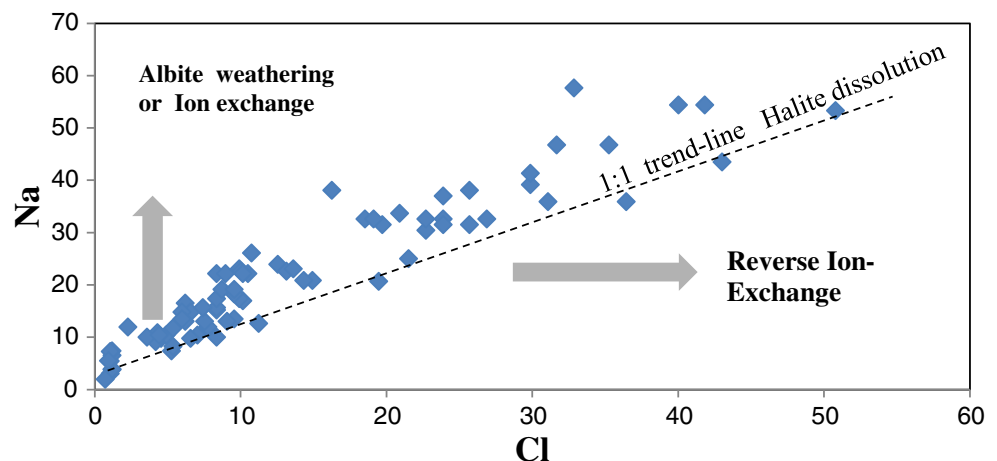
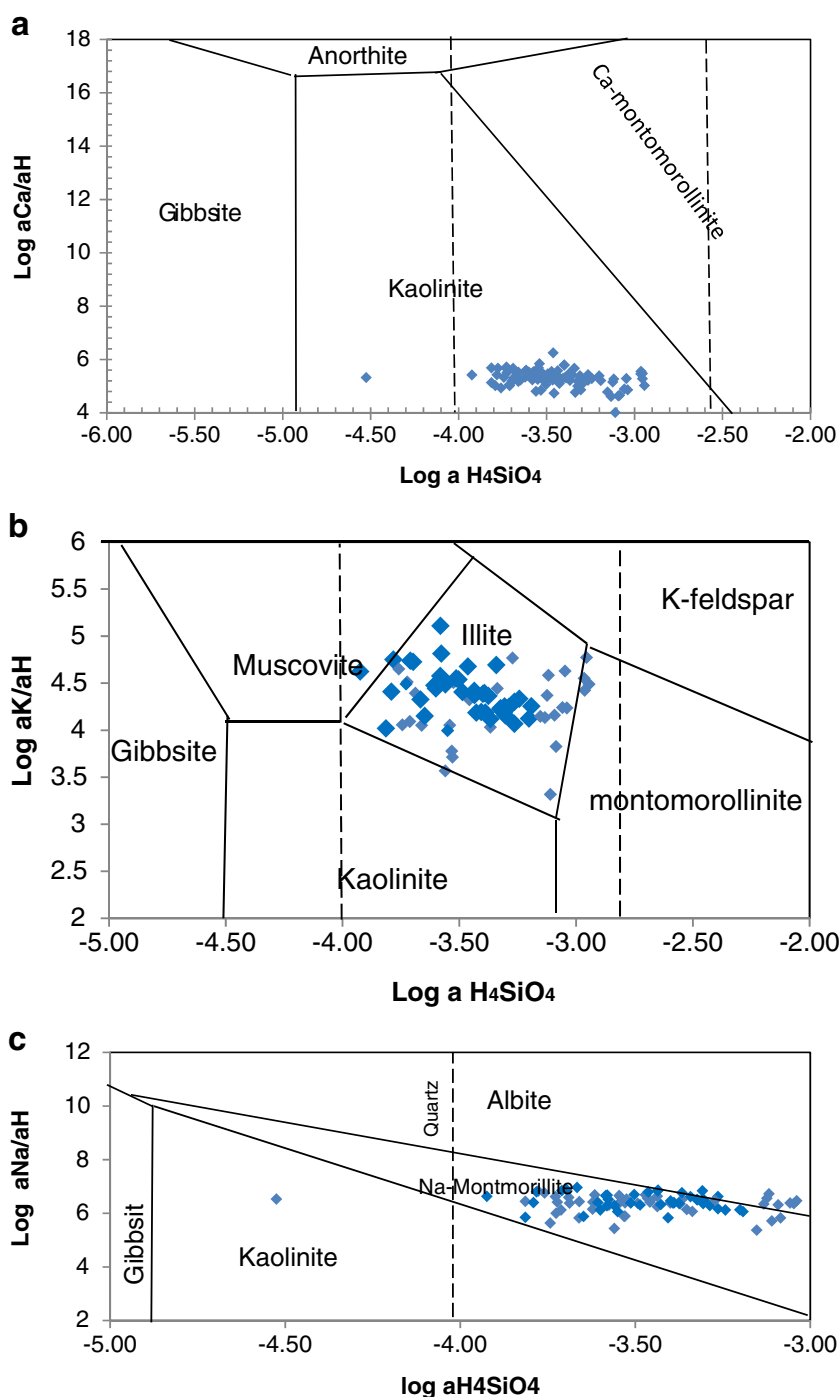


Fig. 12 Stability field of **a** Ca–Al silicate phases, **b** Na–Al silicate phases, and **c** K–Al silicate phases relative to groundwater samples. Most groundwater samples appear to lie at/or close to equilibrium with montmorillonite, kaolinite and illite



The second source of sulfate is atmospheric deposition, where $\delta^{34}\text{S}$ values vary from 8.5 to 13.2 ‰; ^{18}O (SO_4) values vary from 11.1 to 12.7 ‰, emphasizing the process of water recharge from recent Nile water to the Quaternary aquifer. The third source is from leaching and dissolution of sulfate from the Quaternary aquifer, where $\delta^{34}\text{S}$ values vary from 13.7 to 16.8 ‰; ^{18}O (SO_4) values vary from 11.1 to 16.9 ‰. Two samples plot close to the Miocene field indicating the upward contribution from the Miocene aquifer.

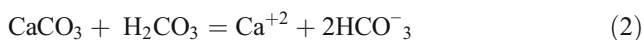
Mechanisms of the hydrogeochemical evolution

The general ranges of the chemical parameters for water from the Quaternary aquifer (Table 2) are as follows: electric conductance, 499–9200; pH, 7.4–8.84; sodium, 45–1453 mg/l; potassium, 1–28 mg/l; calcium, 8–492 mg/l; magnesium, 2–247 mg/l; bicarbonate, 173–666 mg/l; sulfate, 12–1865 mg/l; nitrate, 0–297 mg/l; and silica, 2–70 mg/l. A Na^+ -normalized Ca^{++} VS HCO_3^- plot (Fig. 10) (Gaillardet et al. 1999) shows

Table 3 Results of the inverse modeling for the first flow path

Constraints	Initial (Nile water)	Final (73)	Mineral phases	Δ phase mole transfers				
pH	8.08	8.84	Albite	1.158	11.202	6.74	5.78	11.2
TDS	244	463	Biotite	0.02063	–	–	–	–
Ca	33.3344	20.83	Calcite	–0.40867	–13.824	–0.303	–0.303	–0.3
Mg	17.719317	7.594	Dolomite	–0.1768	–0.26	–0.026	–0.26	–0.2
Na	36.666	125	Gypsum	–0.01799	0.511	0.511	0.511	0.511
K	3	2	K-mica	1.069	–	–	–	–
HCO ₃	176.859	317.62	NaCl	–0.3641	0.777	0.77718	0.777	0.777
Cl	29.6625	38.13	Goethite	–0.0037	0.00229	0.00229	0.00229	0.0023
SO ₄	22.790	47.94	Illite	–1.9	–	–	–	–
SiO ₂	4.33	19.44	Kaolinite	–	–	–	–2.89	13.521
Al	0.853	0.0446	Na-mont	–	13.52	–2.89	–	–16.41
Fe	0.35	0.318	CO ₂ gas	–	18.78	5.26	5.26	5.26
			Anorthite	–	13.52	–2.89	–	–
			SiO ₂	–	–	–9.19	–2.89	–

that all groups of samples plot in and between the fields of evaporite dissolution and silicate weathering. These processes were emphasized by the relationship between Na⁺ and Cl[–] (Fig. 11) showing that some samples plot along the 1:1 trend-line, indicating that halite dissolution is responsible for increased sodium, whereas most of the samples lie above the equi-line and they are typically interpreted as Na⁺ released from a silicate weathering reaction (Meybeck 1987) or due to returned irrigation water. The major component activities of the water samples plot on stability field diagrams of the Na⁺₂O–SiO₂–Al₂O₃–H₂O, K₂O–SiO₂–Al₂O₃–H₂O and Ca⁺⁺O–SiO₂–Al₂O₃–H₂O systems. In these diagrams (Fig. 12a–c), most groundwater samples appear to lie at/or close to equilibrium with montmorillonite, kaolinite, and illite. Such clay minerals are quite common in the local soils (El Nahry 2007). The behavior of carbonate minerals in a near surface environment is primarily controlled by the equilibrium reaction:

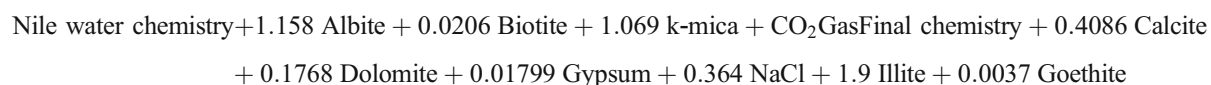


Any process that increases the amount of CO₂ promotes the production of carbonic acid and therefore the system shifts to use up the increased carbonic acid and starts to dissolve calcite. So as the CO₂ increases, the reaction shifts to calcite dissolution. On the other hand, any increase of calcium or bicarbonate shifts the reaction to precipitate calcite. In the Quaternary aquifer, the released bicarbonate and calcite from silicate weathering and evaporite dissolution shift the reaction to calcite precipitation.

Hydrogeochemical inverse modeling

The results of the geochemical modeling (Netpath-win), the water-rock and mass-transfer reactions for two hydrological flow paths, are represented in the following chemical reaction (Tables 3 and 4):

The first flow path (Fig. 1):



The second flow path (Fig. 1):

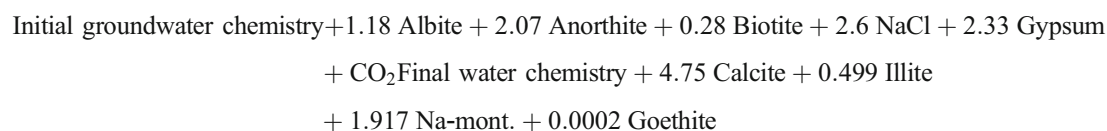


Table 4 Results of the inverse geochemical model for the second flow path

Constraints	Initial	Final	Mineral Phases	Δ phase mole transfers
pH	8.17	8.09	Albite	1.10841
TDS	1492	2551.405	Anorthite	2.13121
Ca	79.169	104.17	Biotite	0.28339
Mg	20.25	104.17	Calcite	-4.75369
Na	420	750	Goethite	-0.00021
K	7	10	NaCl	2.49962
HCO ₃	537.71	375.3745	Illite	-0.49332
Cl	339	656.8125	Gypsum	2.33823
SO ₄	232.66	702.024	Na-mont	-1.93963
SiO ₂	25.6	1.8		
Al	0.214	0.01		
Fe	0.0145	0.004		

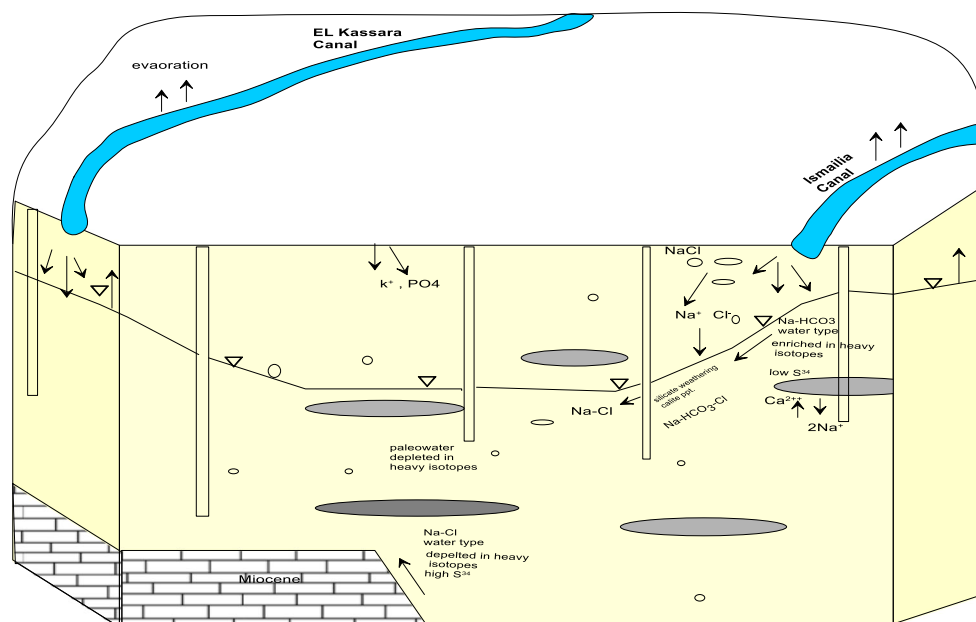
The model shows the incongruent dissolution of silicate minerals, the precipitation of clay minerals and calcite in the Quaternary aquifer. Based on geological, structural, hydrochemical, and isotopic data, a conceptual model for the Quaternary aquifer has been proposed (Fig. 13). The model summarizes the sources of waters and the hydrochemical processes in the aquifer.

Conclusion

Three different sources of water and solutes in the aquifer were investigated including the following: recent

recharge by Nile water at the recharge area which is enriched in heavy isotopes and old recharge by Nile water which is more developed and depleted in heavy isotopes and a minor contribution comes from the underlying Miocene aquifer due to excessive pumping, which is the most enriched water in $\delta^{34}\text{S}$ and $\delta^{18}\text{O}$ of sulfate. The $\delta^{18}\text{O}$ versus Cl relationship reflects that different hydrogeochemical processes account for the chemistry of the groundwater. They comprise the following: leaching and dissolution of salts, evaporation of shallow groundwater, and recharge from surface water. Sodium and calcium ions in the Quaternary aquifer are coming from the incongruent dissolution of

Fig. 13 Conceptual model for the Quaternary aquifer, illustrating the different geochemical processes



plagioclase (albite and anorthite) to form clay minerals which increase along the flow path. Additional potential sources of Na^+ come from evaporite deposits and cation exchange of divalent cations for Na^+ . Magnesium and potassium ions result from the incongruent dissolution of biotite, K-feldspars, and ferromagnesian minerals (pyroxenes and amphiboles) or dolomite/high magnesium calcite.

Acknowledgments The authors would like to thank The Egyptian Cultural and Educational bureau in Washington DC for the funds provided to complete this study.

References

- Ahmed MA, Abdel Samie SG, Badawy HA (2013) Factors controlling mechanisms of groundwater salinization and hydrogeochemical processes in the Quaternary aquifer of the Eastern Nile Delta. *Egypt Environ Earth Sci* 68:369–394
- Al-Gamal SA, Korany EA, Awad SA, Ahmed MA, Abdelwahab S (2005) Recharge mechanisms for the Quaternary and the Miocene aquifers, East Cairo District, Egypt, using conventional and non conventional techniques. *Isotope & Rad Res* 37(3):711–735
- Clark ID, Fritz P (1997) *Environmental isotopes in hydrogeology*. Lewis Publishers, New York
- Dahab KA, El Abd EA, Fattah MK, El Osta MM (2007) Assessment of groundwater problems of the Quaternary aquifer in the area between El Salhia El Gidida-Abu Sweir, East Nile Delta. *Egypt GREMNA* 2: 329–353
- El Dairy MD (1980) Hydrogeological studies on the eastern part of Nile Delta using isotope techniques. A master thesis submitted to Zagazig Uni., Egypt
- El Nahry AH (2007) Using geostatistical analysis and spectral signature for identifying shale distribution and type in El-Salhia project, Ismaillia, Egypt. *Int J Geol* 1:22–26
- Gad MI (1995) Hydrogeological studies for groundwater reservoirs, east of the Tenth of Ramadan city and vicinities. a master thesis submitted to Ain Shams Uni, Cairo, Egypt
- Gaillardet J, Dupre B, Louvat P, Allegre CJ (1999) Global silicate weathering and CO_2 consumption rates deduced from the chemistry of large rivers. *Chemical geology*. 159:3–30
- Gu A (2005) Stable isotope geochemistry of sulfate in groundwater of Southern Arizona: implications for groundwater flow, sulfate sources, and environmental significance. A PhD dissertation submitted to the University of Arizona, Geosciences
- Güler C, Thyne GD (2004) Delineation of hydrochemical facies distribution in a regional groundwater system by means of fuzzy c-means clustering. *Water Resour Res* 40. doi:10.1029/2004WR003299
- Hamza MS, Aly AI, Swailem FM, Nada A (1987) Environmentally stable isotopes and groundwater recharge in the eastern Nile delta. *International Journal of Water Resources Development* 3(4):228–232
- Meybeck M (1987) Global chemical weathering from surficial rocks estimated from river dissolved loads. *American Journal of Science*. 287:401–428
- Mook WG (2000) *Environmental isotope in the hydrological cycle; principles and application*, vol IHP-V, Technical Documents in Hydrology | No. 39. UNESCO/IAEA, Paris
- Moussa BM (1990) Petrology and soil genesis of the surface Quaternary deposits, East of the Nile Delta, Egypt. A PhD thesis submitted to the Uni. of Ain shams. Faculty of sci.
- Murray KS (1996) Hydrology and geochemistry of thermal waters in the Upper Napa valley, California. *Ground Water* 34(6):1115–1124
- Rosen M, Jones S (1998) Controls of the chemical composition of groundwater from alluvial aquifers in the Wanaka and Wakatipu basins, central Otago. *New Zealand Hydrogeology J* 6:264–281
- Salem WM (1996) Application of isotopic and hydrochemical techniques to study groundwater in eastern Nile Delta and assessment of pollution in Lake Manzala. A PhD thesis submitted to Cairo Uni. Fac. of Engineering
- Salem WM, Sadek MA (2006) Chemical and isotopic signature for mapping zones of Sea water intrusion and residual saline pockets in coastal aquifers of the Egyptian Nile Delta. *Arab J Nucl Sci Appl* 39:111–127
- Salluma M (1983) Hydrogeological and hydrochemical studies east of the Nile Delta. A PhD dissertation submitted to Ain Shams University, Egypt
- Sharif MU, Davis RK, Steele KF, Kim B, Kresse TM, Fazio JA (2008) Inverse geochemical modeling of groundwater evolution with emphasis on arsenic in the Mississippi River Valley alluvial aquifer, Arkansas (USA). *Hydrogeology J*. 350:41–55